

# Normal-state transport properties of $\text{Ba}_{1-x}\text{K}_x\text{BiO}_3$ crystals

Y. Nagata<sup>a,\*</sup>, A. Mishiro<sup>a</sup>, T. Uchida<sup>b</sup>, M. Ohtsuka<sup>b</sup>, H. Samata<sup>c</sup>

<sup>a</sup>College of Science and Engineering, Aoyama Gakuin University, Chitosedai, Setagaya, Tokyo 157, Japan

<sup>b</sup>Tokyo Institute of Polytechnics, Iiyama, Atsugi, Kanagawa 243, Japan

<sup>c</sup>Faculty of Mercantile Marine Science, Kobe University of Mercantile Marine, 5-1-5 Fukaeminami, Higashinada, Kobe 658-0022, Japan

Received 12 May 1999; accepted 14 May 1999

## Abstract

The normal-state transport properties of  $\text{Ba}_{1-x}\text{K}_x\text{BiO}_3$  crystals with a wide range of potassium compositions ( $0 \leq x \leq 0.62$ ) were studied. Although the host material  $\text{BaBiO}_3$  has a monoclinic structure, the system changes from a monoclinic to an orthorhombic structure with a small doping of potassium ( $0 \leq x < 0.35$ ) and behaves similar to a doped semiconductor, without exhibiting superconductivity. In the composition range, holes are majority carriers in the transport phenomena. When  $x$  exceeds a critical value ( $\sim 0.35$ ), the system goes into a cubic superconducting phase with a single metallic band. The vicinity of the critical composition transport phenomena is easy to understand assuming the existence of two conducting channels that are made up of metallic and semiconducting phases. Maximum  $T_c$  exceeding 30 K was observed at  $x \sim 0.4$ , where carrier density was at its maximum. Overdoping with potassium suppresses superconductivity. In the metallic composition of  $x > 0.45$ , transport seems to correlate with the phonon mode with an energy distribution of 15–43 meV. © 1999 Elsevier Science Ltd. All rights reserved.

**Keywords:** A. Oxides; A. Superconductors; B. Crystal growth; D. Transport properties

## 1. Introduction

Among oxide superconductors that do not contain copper,  $\text{Ba}_{1-x}\text{K}_x\text{BiO}_3$  (hereafter referred to as BKBO) exhibits the highest superconducting transition temperature, exceeding 30 K at the optimal doping level ( $x \sim 0.4$ ) [1,2]. The most remarkable feature of BKBO, unlike high- $T_c$  cuprates, is its isotropic crystal structure without any metal-oxygen superconducting layers. This structure is believed to play a key role in the production of high-temperature superconductivity. The parent compound  $\text{BaBiO}_3$  ( $x = 0$ ) has a monoclinic crystal structure with a breathing- and a tilting-mode lattice distortion of  $\text{BiO}_6$  octahedra [3], and it shows semiconducting behavior despite the theoretical calculation predicting metallic behavior [4]. The distortion produces inequivalent Bi sites and is believed to cause a possible valence disproportionation (or charge density wave; CDW) of  $\text{Bi}^{3+}$  and  $\text{Bi}^{5+}$ . The breathing-mode distortion disappears at  $x \sim 0.1$ , and the material changes into an orthorhombic structure. The semiconducting behavior persists in the orthorhombic

phase. A cubic metallic superconducting phase is established at a potassium content of  $x \sim 0.35$  [3]. While the maximum superconducting transition temperature ( $T_c$ ) is attained near  $x = 0.4$ , further doping with potassium causes a decrease in the superconducting transition temperature [5]. Superconductivity is observed up to  $x \sim 0.5$ , which has been thought to be the solubility limit of potassium [3]. The majority carriers, which contribute to transport behavior, are known to be electrons in the metallic phase despite the substitution of divalent barium by monovalent potassium.

As BKBO has no local magnetic moment, any magnetic pairing mechanisms that may explain the mediation of superconductivity in cuprate superconductors does not hold in BKBO. Recent experimental studies on single crystalline specimens elucidated the superconductivity of BKBO [6–10]. Moreover, measurements of transport properties [6,9–15], magnetic properties [12,16–20], pressure effect [21], photo-electron spectroscopy [22], and tunneling spectroscopy [23] revealed that a phonon-mediated pairing mechanism plays a key role in the superconductivity of BKBO. However, in spite of extensive studies about

\* Corresponding author.

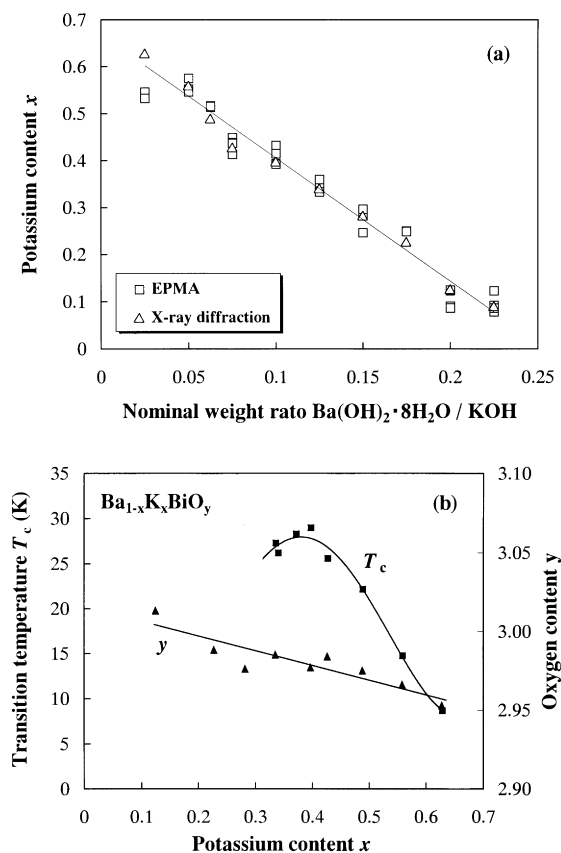


Fig. 1. (a) Potassium content  $x$  of  $\text{Ba}_{1-x}\text{K}_x\text{BiO}_3$  crystals as a function of weight ratio  $\text{Ba(OH)}_2 \cdot 8\text{H}_2\text{O} / \text{KOH}$  in nominal composition. (b) Oxygen content and superconducting critical temperature of the crystals as a function of potassium content. The solid lines are only a visual guide.

superconductivity, the normal-state transport properties of BKBO are still unclear, and some obscure points including semiconductor-metal transition remain to be clarified. In order to understand the nature of BKBO, it is essential to clarify the normal-state transport properties. Although studies on transport properties have been performed on single crystals and thin films [6,9–15,24], there are some discrepancies in the results of resistivity and Hall effect measurements. This discrepancy seems to be caused by a difference in crystal quality and indistinct composition, including the oxygen content of the specimens. In order to have a better understanding of the normal-state transport properties of BKBO, it is necessary to perform experiments for high-quality crystals with a distinct composition. Moreover, as a phonon-mediated mechanism is thought to play an important role in the superconductivity of BKBO, transport behavior must be investigated by taking account of electron-phonon interaction. Although it was a difficult task to control the potassium and oxygen content and to establish the homogeneity of BKBO crystals, we have opened a route

that can control the composition and quality of BKBO crystals [9]. In this study, normal-state transport properties were measured for crystals with various potassium contents and distinct oxygen content, and the transport behaviors were investigated in detail.

## 2. Experiment

BKBO crystals were grown by the electrochemical method developed by Norton [25]. Details about crystal growth have been described in previous papers [6,9]. Raw materials,  $\text{Ba(OH)}_2 \cdot 8\text{H}_2\text{O}$  (98%) and  $\text{Bi}_2\text{O}_3$  (99.9%), were dissolved into liquid KOH (semiconductor grade) in a platinum crucible at  $210^\circ\text{C}$  in a flowing mixed gas of oxygen and nitrogen. To obtain crystals with various potassium contents, the weight ratio  $\text{Ba(OH)}_2 \cdot 8\text{H}_2\text{O} / \text{KOH}$  was varied from 0.025 to 0.225. The crystals were grown at  $210^\circ\text{C}$  for 40 h at an applied voltage of 0.4 V. Crystals were then removed from the KOH solution, immediately after the applied voltage was turned off, and were washed using distilled water and ethanol. Crystals with a composition of  $x = 0$ , which corresponds to  $\text{BaBiO}_3$ , were grown by cooling a melt of polycrystalline specimen in an alumina crucible from  $900$  to  $600^\circ\text{C}$  at a rate of  $2^\circ\text{C}/\text{h}$ .

Powder X-ray diffraction was performed by using  $\text{CuK}\alpha$  radiation, and the refinement of the diffraction data was performed for all crystals in order to evaluate crystal structure. The composition of the crystals was determined by electron probe microanalysis (EPMA). Potassium contents were also determined by the relation  $a = 4.3548 - 0.1743x$  between pseudo-cubic lattice constant  $a$  and potassium content  $x$ , which was discovered by Pei et al. [3] during their neutron diffraction study of polycrystalline specimens. The oxygen contents of the crystals were determined by iodometric analysis. Transport properties were measured at temperatures between 10 and 300 K by a DC four-probe and two-probe methods on the [100] plane of the crystals with a rectangular shape. Hall-effect measurements were performed with the four-probe method at temperatures between 77 and 300 K in applied fields from 0 to 8 kOe using an electromagnet. The electrical contacts that were used for transport measurements were established by attaching gold leads onto a crystal surface by silver paint with subsequent annealing in oxygen at  $400^\circ\text{C}$  for 4 h.

## 3. Results and discussion

### 3.1. Temperature dependence of resistivity

The potassium contents of the crystals that were grown in this study are shown in Fig. 1(a) as a function of the nominal weight ratio of  $\text{Ba(OH)}_2 \cdot 8\text{H}_2\text{O}$  to KOH. The potassium content decreased linearly when the weight ratio increased. The potassium contents estimated from the lattice parameter of the crystals were in agreement with those determined by

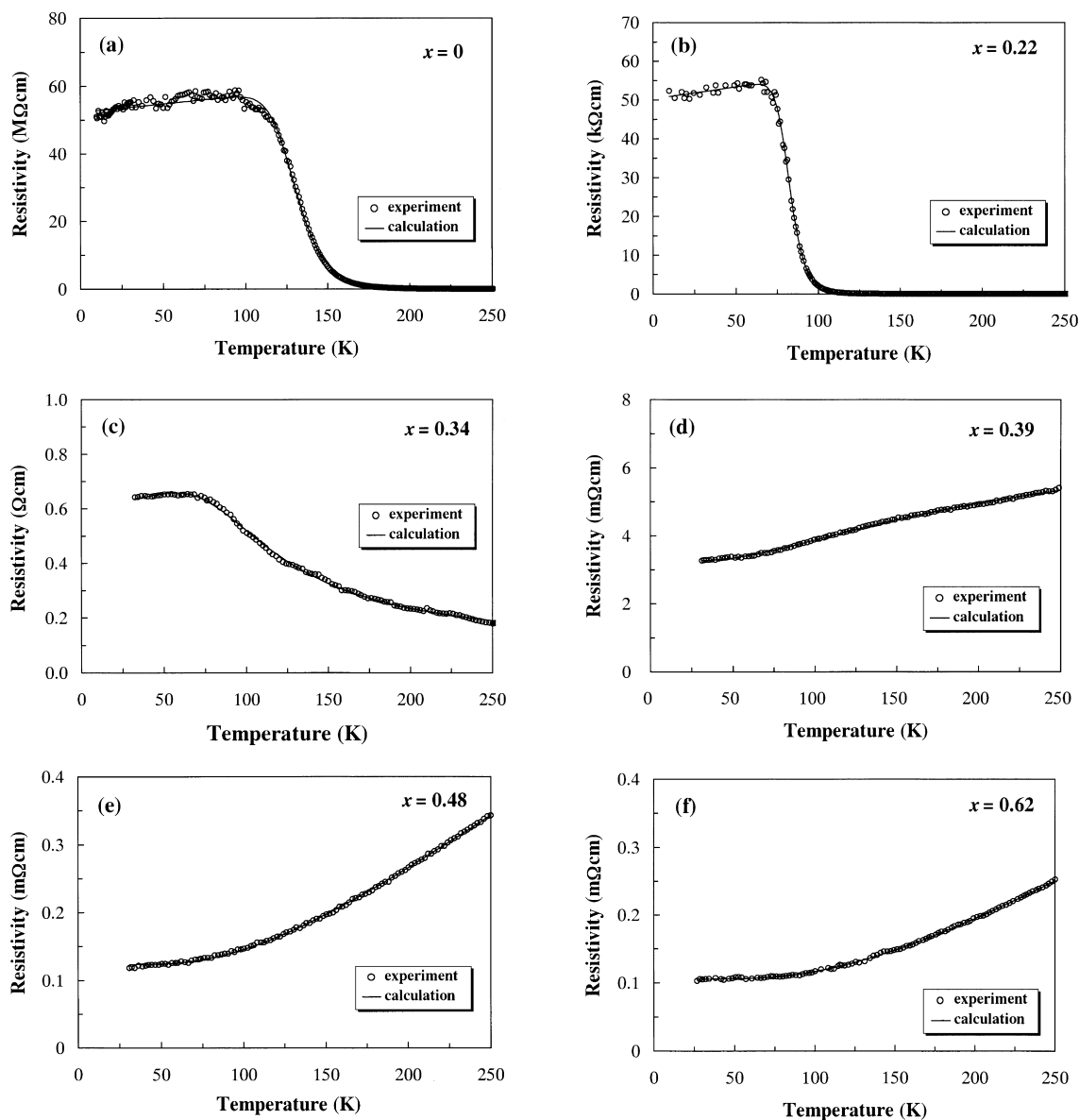


Fig. 2. The temperature dependence of resistivity for the crystals with: (a)  $x = 0$ ; (b)  $x = 0.22$ ; (c)  $x = 0.34$ ; (d)  $x = 0.39$ ; (e)  $x = 0.48$ ; and (f)  $x = 0.62$ . The solid lines show the calculation results.

microanalysis using EPMA. Attempts to dope with potassium of  $x > 0.62$  were unsuccessful. The oxygen content and superconducting transition temperature  $T_c$  of crystals with various potassium compositions are shown in Fig. 1(b). The oxygen content in the crystals decreased as the potassium content increased. As the decrease in oxygen content was very small ( $\sim 4.55 \times 10^{-3}/x$ ), the crystals grown by electrochemical deposition are thought to contain enough oxygen to cause superconductivity. Therefore, although there is a potential that a little decrease in oxygen content helps to compensate a charge unbalance caused by

potassium doping, the electrical neutrality in the crystal will be basically attained by a change in the atomic valence of bismuth ions. Superconductivity was observed for crystals with a potassium content above  $x \sim 0.3$ . As shown in the figure, superconducting transition temperature  $T_c$  tends to increase initially as the potassium content increases; however, it decreases after it reaches a maximum at about  $x = 0.4$ . Superconducting transition can still be observed for a crystal with  $x = 0.62$  ( $T_c \sim 8.5$  K).

The typical temperature dependence of resistivity  $\rho(T)$  for crystals with various amounts of potassium is shown in

Table 1

The parameters used for fitting Eq. (1) to the data of resistivity measurements for crystals with potassium concentrations of  $0 \leq x \leq 0.28$

$x$	$\rho_0$ (k $\Omega$ cm)	$\alpha$ ( $\Omega$ cm/K)	$\sigma_s$ (S cm $^{-1}$ )	$E_s$ (meV)
0.00	5232	49568	0.063	168
0.11	54	114	578	173
0.23	53	63	2287	131
0.28	44	22	45	119

Fig. 2. The behavior of  $\rho(T)$  varies remarkably when the potassium doping level is increased. The  $\rho(T)$  of crystals with potassium contents of  $x < 0.3$  (Fig. 2(a) and (b)) show a temperature dependence similar to that of doped-semiconductors without exhibiting superconductivity; the resistivity increases when the temperature decreases, tending to be saturated at very low temperatures. Crystals with a composition of  $0.3 < x < 0.45$  (Fig. 2(c) and (d)) show a superconducting transition at low temperatures. However, semiconductor-like behavior is still observed in the  $\rho(T)$  of crystals with compositions near  $x = 0.34$ . Crystals with a composition of  $x = 0.39$  show a peculiar temperature dependence; the resistivity decreases as the temperature decreases, and a hump is observed in the  $\rho(T)$  curve at temperatures between 100 and 200 K. An almost linear temperature dependence can be seen in crystals with a composition of  $x = 0.42$  above 100 K, which have the highest  $T_c$  ( $\sim 30$  K). Crystals with a potassium content of  $x > 0.45$  (Fig. 2(e) and (f)) exhibit simple metallic behavior, but superconductivity is observed up to  $x = 0.62$  ( $T_c = 8.5$  K). The behavior resembles the features of conventional metallic superconductors.

### 3.1.1. Behaviors in low potassium compositions

The  $\rho(T)$  of a BaBiO<sub>3</sub> ( $x = 0$ ) crystal (Fig. 2(a)) is similar

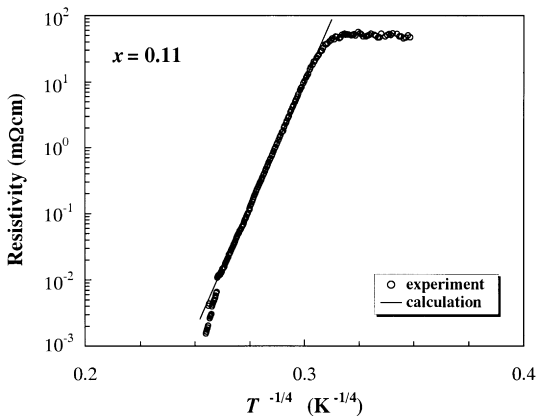


Fig. 3. The  $T^{-1/4}$  dependence of resistivity for a crystal with  $x = 0.11$ . The solid line shows the result of fitting using the formula  $\rho = \rho_0 \exp(T_0/T)^{1/4}$ .

to those of the doped semiconductors. In general, the resistivity of typical semiconductors is proportional to the inverse of the number of carriers that are excited across an energy gap and is represented by  $\rho_s(T) = \rho_s[\exp(E_s/k_B T) + 1]$ , where  $E_s$ ,  $k_B$ , and  $\rho_s$  are the excitation energy, Boltzmann's constant, and proportional coefficient, respectively. The  $\rho(T)$  of crystals with a composition of  $x < 0.3$  can be explained by a parallel resistor model given by

$$\rho(T) = \frac{1}{(\rho_0 + \alpha T)^{-1} + \rho_s(T)^{-1}}, \quad (1)$$

where  $\rho_0$  and  $\alpha$  are the residual resistivity and temperature coefficient, respectively. Resistivity that cannot be explained by a semiconducting component has been ascribed to  $\rho_0 + \alpha T$ . When the temperature decreases, the conduction in the semiconducting part freezes, and  $\rho_0 + \alpha T$  plays a dominant role in the resistive behavior. The result obtained by fitting Eq. (1) to the  $\rho(T)$  of BaBiO<sub>3</sub> crystal is shown in Fig. 2(a) by a solid line. The  $\rho(T)$  is explained effectively by Eq. (1) in the whole temperature range measured. The excitation energy  $E_s$  of 0.17 eV was obtained by fitting the above equation to the data. This value is slightly lower than that ( $\sim 0.24$  eV) obtained by Takagi et al. [26] from resistivity data at high temperatures between 150 and 800 K and the value (0.21–0.27 eV) obtained by Hashimoto et al. [27] at temperatures between 100 and 280 K. The discrepancy in these results is thought to be caused by the formula used for fitting. Takagi et al. used a simple Arrhenius-type formula  $\rho(T) = A \exp(E_s/k_B T)$  in order to evaluate  $E_s$ . When the formula was used to fit the linear part of the  $\rho(T^{-1})$  curve obtained in this study, an  $E_s$  of 0.21 eV was obtained. This value is consistent with those obtained by Takagi et al. and Hashimoto et al. The semiconducting nature of BaBiO<sub>3</sub> seems to be caused by a possible valence fluctuation of bismuth ions that is due to a breathing and tilting mode lattice distortion of the BiO<sub>6</sub> octahedra, and the charge fluctuation creates a gap in the Bi 6s band. Namatame et al. have revealed the existence of a gap opening at the Fermi level through a study of photo-electron spectroscopy for BKBO crystals with various potassium compositions [22].

The  $\rho(T)$  curves for crystals with potassium contents of up to  $x \sim 0.3$  can also be explained by Eq. (1). An activation-type conduction seems to be dominant in normal-state electrical conduction at temperatures above  $\sim 100$  K. However,  $\rho(T)$  changes its behavior at temperatures below 100 K, and after reaching its maximum it tends to decrease slightly as the temperature decreases. Presumably, at low temperatures, a crossover from semiconducting conduction to another type of conduction occurs. The results of fitting Eq. (1) to the data are shown in Fig. 2(b) by a solid line, and the parameters used for fitting are listed in Table 1, where  $\sigma_s = \rho_s^{-1}$ . Excitation energy  $E_s$  decreases as the potassium content increases. This fact indicates that a reduction of the semiconducting band-gap takes place by potassium doping.

Table 2

The parameters used for fitting Eq. (2) to the data of resistivity measurements for crystals with potassium concentrations of  $0.34 \leq x \leq 0.42$

$x$	$\rho_0$ (mΩ cm)	$\sigma_s$ (S cm <sup>-1</sup> )	$\alpha_m$	$E_s$ (meV)	$E_{m1}$ (meV)	$E_{m2}$ (meV)
0.34	632	21.9	$1.44 \times 10^{-1}$	27.1	15.7	19.6
0.39	3.26	228	$1.64 \times 10^{-3}$	30.4	16.0	18.4
0.42	1.92	276	$5.48 \times 10^{-5}$	29.9	15.4	25.1

The reduction of the band-gap was also observed in a study of X-ray photoelectron spectroscopy (XPS) for BKBO crystals [22], which are the same crystals as those used in this study.

As shown above, the  $\rho(T)$  curve of crystals with a potassium content of  $x \sim 0.1$  can be fitted basically by using Eq. (1) in the whole temperature range measured. However, as shown in Fig. 3, the resistivity of a crystal with  $x = 0.11$  shows  $T^{-1/4}$  dependence at temperatures between 116 and 219 K. This fact implies that variable range hopping (VRH) conduction [28], which is represented by the formula  $\rho(T) = \rho_0 \exp[(T_0/T)^{1/4}]$ , plays a role in the transport behavior at this composition. Hellman et al. also noted the existence of VRH for a crystal with  $x = 0.13$  [11]. The value  $T_0 = 1.15 \times 10^9$  K obtained in this study is consistent with that reported by Hellman et al. As this composition corresponds to that of the phase boundary between monoclinic and orthorhombic phases, and the difference in crystal structure between these phases is only a breathing mode distortion of BiO<sub>6</sub> octahedra, two phases may possibly coexist in a crystal with a composition at the phase boundary. The coexistence of two phases will introduce a modulation of the periodic potential in the crystal lattice and create localized states at the band-tail near the Fermi level; hence, VRH conduction will occur among these states. Resistivity cannot be explained by VRH or by simple activation-type conduction at low temperatures below  $\sim 100$  K. This indicates that a crossover from VRH to another conduction process occurs at low temperatures. Localization length  $1/\alpha$  and average hopping distance  $R$  can be roughly estimated using the  $T_0$  values and the density of states  $N(E_f)$  at the Fermi level according to the formulas  $T_0 = 24\alpha^3[\pi k_B N(E_f)]^{-1}$  and  $R = (3/8\alpha)(T_0/T)^{1/4}$ , which explain the transport properties of non-crystalline materials [28]. If the value  $T_0 \sim 1 \times 10^9$  K and instead of  $N(E_f)$ , Hall carrier density  $n_H \sim 5 \times 10^{19}$ , which was obtained by the Hall-effect measurement mentioned later, were used,  $(1/\alpha) \sim 2.58 \times 10^{-8}$  cm (or 25.8 nm) and  $R \sim 4.6 \times 10^{-7}$  cm (or 460 nm) were deduced at 200 K. The value of  $R$  is an order of magnitude larger than the lattice spacing ( $\sim 40$  nm), suggesting that a long-range inter-unit-cell hopping conduction takes part in transport behavior at a composition that is near phase boundary ( $x \sim 0.1$ ).

### 3.1.2. Behaviors in intermediate potassium compositions

$\rho(T)$  curves of crystals with compositions of  $0.3 < x <$

0.45 can be explained by the formula:

$$\rho(T) = \frac{1}{\rho_s(T)^{-1} + \rho_m(T)^{-1}} \quad (2)$$

which was used by Hellman et al. [24], in order to explain the transport behaviors of BKBO thin films assuming parallel metallic and semiconducting channels. Here,  $\rho_s(T)$  and  $\rho_m(T)$  are, respectively, the resistivity of the semiconducting channel and the metallic channels as a function of temperature. The metallic channel is responsible for conductivity at lower temperatures, and the semiconducting channel, which freezes at low temperatures, is dominant at higher temperatures. The resistivity  $\rho_m(T)$  of the metallic channel can be ascribed to a scattering of conduction electrons by thermal phonons and is proportional to an integral over the phonon density of state. If the phonon mode has a flat energy distribution from  $E_{m1}$  to  $E_{m2}$ , the  $\rho_m(T)$  can be expressed by

$$\rho_m(T) = \rho_0 + \alpha_m \left[ \frac{E_{m1} - E_{m2}}{k_B} + T \ln \left( \frac{e^{E_{m2}/k_B T} - 1}{e^{E_{m1}/k_B T} - 1} \right) \right] \quad (3)$$

where  $\rho_0$  and  $\alpha_m$  are the residual resistivity and the fitting coefficient, respectively. The results obtained by fitting Eq. (3) to the data are shown in Fig. 2(c) and (d) by solid lines, and the parameters used for fitting are listed in Table 2. The values of  $E_s$  are almost constant ( $\sim 30$  meV) in these compositions. The phase boundary between orthorhombic and cubic phases, which is shown by Pei et al. [3], exists in this composition range. When the doping level of potassium is increased, the semiconducting band-gap disappears due to the suppression of lattice distortion, and a Bi 6s single conduction band seems to be established in the cubic phase. The band appears to be similar to that predicted theoretically for cubic BaBiO<sub>3</sub> by Hamada et al. [29]. Superconductivity appears at the composition of  $x \sim 0.35$ . On the other hand,  $E_m$  takes the value of 15–25 meV. These values are consistent with those obtained for BKBO thin films by Hellman et al. [24].

A similar type of transport behavior, which suggests the existence of two conducting channels, was observed in the related superconductor BaPb<sub>1-x</sub>Bi<sub>x</sub>O<sub>3</sub> by Marx et al. [30]. Although a variety of explanations can be given with regard to the two conducting channels, an inhomogeneous distribution of potassium may introduce two structurally different components into BKBO crystals. The coexistence of the two components may explain the two electrically different

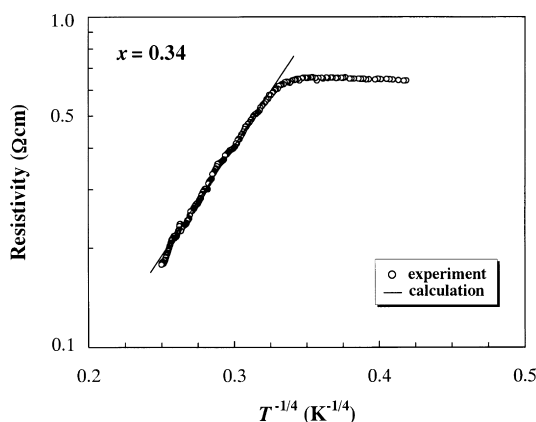


Fig. 4. The  $T^{-1/4}$  dependence of resistivity for a crystal with  $x = 0.34$ . The solid line shows the result of fitting using the formula  $\rho = \rho_0 \exp(T_0/T)^{1/4}$ .

channels. As the potassium content of  $x = 0.3$ – $0.4$  is insufficient for the homogeneous distribution of potassium ions in a Perovskite lattice and the difference between orthorhombic and cubic structures is very small, orthorhombic semiconducting components will persist partially in the cubic metallic phase of these compositions. By using the optical measurement, Karlow et al. observed the persistence of the IR absorption band in the metallic compositions [31]. As the IR absorption band corresponds to an excitation across the band-gap, this suggests the existence of a semiconducting component in crystals with  $x = 0.3$ – $0.4$ . Moreover, Hamada et al. showed that two different Bi–O distances, which are characteristic in the monoclinic phase, exist in BKBO crystals even in these compositions [29]. The existence of different Bi–O distances may be another reason for the formation of the semiconducting channel [31]. These results support the validity of using a two-channel conduction model to explain the transport behavior of BKBO. Although the microscopic origin of the two conducting channels is unclear at present, the characteristic transport properties observed for crystals with  $0.3 < x < 0.45$  can be explained by the parallel conducting channel model. A pseudogap, which was observed in XPS measurements for the same crystals as those used in this study [22], could not be confirmed in the transport measurements that were performed in this study. However, a

Table 3

The parameters used for fitting Eq. (3) to the data of resistivity measurements for crystals with potassium concentrations of  $0.48 \leq x \leq 0.62$

$x$	$\rho_0$ (mΩ cm)	$\alpha_m$	$E_{m1}$ (meV)	$E_{m2}$ (meV)
0.48	0.124	$5.4 \times 10^{-5}$	21.7	26.7
0.56	0.221	$9.4 \times 10^{-6}$	27.6	36.1
0.62	0.106	$2.2 \times 10^{-5}$	28.1	42.8

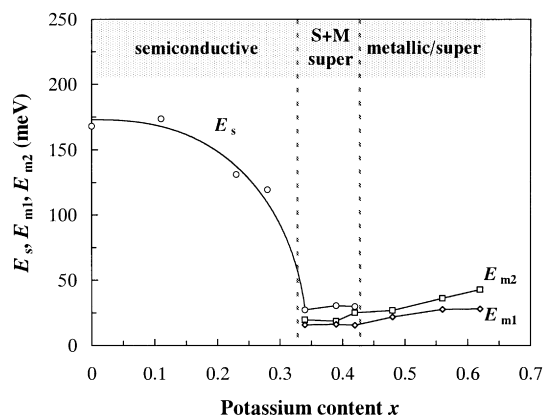


Fig. 5. Parameters  $E_s$ ,  $E_{m1}$ , and  $E_{m2}$  as a function of potassium content  $x$ , which were obtained by an analysis of the temperature dependence of resistivity, as shown in Fig. 2.

neutron-diffraction study for a specimen with a composition of  $\text{Ba}_{0.6}\text{K}_{0.4}\text{BiO}_3$  revealed the existence of a dynamic lattice distortion [32]. Presumably, to stabilize the lattice distortion the state density at the Fermi level would decrease for reducing the energy of electrons; and this might be a reason of the formation of the pseudogap.

Although the  $\rho(T)$  curve of a crystal with  $x = 0.34$  could be explained by Eq. (2), as shown in Fig. 4, the  $\rho(T)$  seems to depend on  $T^{-1/4}$  at temperatures between 95 and 250 K. This fact may suggest that a VRH conduction plays a role in crystals with  $x \sim 0.35$ . Dabrowski et al. [33] also observed the  $T^{-1/4}$  dependence of resistivity in a polycrystalline specimen with  $x = 0.35$ . As this composition corresponds to a critical concentration for the phase transition from an orthorhombic to a cubic structure, there is a high potential that these phases coexist in the crystal. In this case, a randomness may be introduced to the crystal lattice, and VRH conduction will take place.

### 3.1.3. Behaviors in high-potassium compositions

The metallic behaviors that were observed in crystals with  $x > 0.45$  can be explained by Eq. (3). The fitting results are shown in Fig. 2(e) and (f) by solid lines, and the fitting parameters for crystals with various amounts of potassium are listed in Table 3.  $E_m$  has a value that is distributed in a range from 22 to 43 meV. This indicates that the phonon mode, which affects transport behavior, has an energy distribution from 22 to 43 meV. According to the neutron diffraction study on BKBO polycrystal, it is revealed that the spectrum of acoustic-phonon distributes in an energy range of 10–50 meV, and that of optical-phonon, which is due to oxygen-breathing vibrations, distributes at energies from 50 to 80 meV [34]. The value of  $E_m$  obtained in this study are consistent with the phonon spectrum distribution (10–80 meV) observed in neutron diffraction measurement, 15–70 meV obtained by tunneling spectroscopy [23,35], and the values of 27 and 58 meV obtained by an analysis

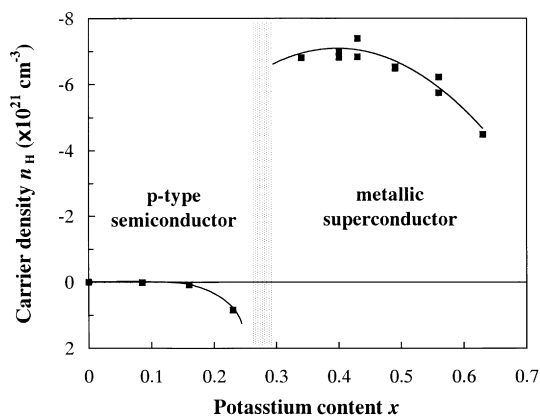


Fig. 6. Hall densities  $n_H$  at 300 K as a function of potassium content  $x$ . The solid lines are only a visual guide.

of resistivity measurement for a metallic crystal [36]. This suggests that electron-phonon interaction plays a key role in the transport phenomena and the superconductivity of BKBO.

Parameters  $E_s$ ,  $E_{m1}$ , and  $E_{m2}$ , which were obtained by an analysis of  $\rho(T)$  curves for crystals with various potassium compositions, are shown in Fig. 5 as a function of potassium content  $x$ . In accordance with potassium doping, the semi-conducting band-gap  $E_s$  decreases monotonically and almost disappears at  $x \sim 0.35$ , indicating the formation of a Bi 6s single metallic band. This composition might be a critical composition for the metal-insulator transition. On the other hand,  $E_m$ 's for crystals with metallic compositions increase slightly upon increasing potassium doping. This may suggest a dominant contribution of electron-phonon interaction in the transport behavior of metallic BKBO.

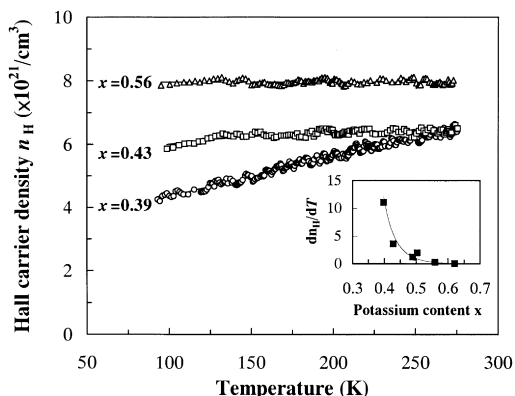


Fig. 7. The temperature dependence of Hall carrier density  $n_H$ . Solid lines show the results of fitting using  $n(T) = n_m + n_s / [\exp(E_s/k_B T) + 1]$  assuming semiconducting and metallic components. The inset is the potassium content dependence of the slope of the straight lines fitted for the data.

### 3.2. The behavior of carriers: Hall-effect measurements

In order to investigate the behavior of carriers contributing to the transport behavior of BKBO, Hall-effect measurements were performed at temperatures between 77 and 300 K for the same crystals as those used in the resistivity measurements. Hall densities  $n_H$  obtained at 300 K are shown in Fig. 6 as a function of potassium content  $x$ . In the  $\text{BaBiO}_3$  ( $x = 0$ ) crystal, Hall coefficient  $R_H$  has a positive sign, which indicates that the holes are the majority carriers in electrical conduction. When potassium is doped into the crystal,  $n_H$  increases by a magnitude of three at a composition of  $x = 0.23$ . Hall voltage was not detected, even with a sensitivity of 1 nV, for crystals with compositions of  $0.23 < x < 0.34$ . Hall effect seems to be extremely small in these crystals. It is noted that a peculiar magnetically induced voltage, different from the Hall voltage, was observed for crystals in this composition range. The reason for this behavior, which disturbed the Hall-effect measurement, is unclear at present.

The sign of Hall coefficient  $R_H$  suddenly changes from positive to negative at compositions near  $x = 0.34$ , which is close to the critical composition of the phase boundary between orthorhombic and cubic structures. This composition also corresponds to that of the metal-insulator transition observed in the resistivity measurements. These facts suggest that the phase transition at  $x \sim 0.35$  has a significant effect on the electronic structure of BKBO.

All crystals with compositions of  $x \geq 0.34$  have negative  $R_H$ , which indicates that electrons are the majority carriers in electrical conduction and play an important role in the superconductivity of BKBO. Hall density  $n_H$  decreases monotonically with an increase in potassium content after reaching a maximum ( $-7.0 \times 10^{21} \text{ cm}^{-3}$ ) at  $x \sim 0.4$ . The  $n_H$  of  $-7.0 \times 10^{21} \text{ cm}^{-3}$  corresponds to a carrier density of  $\sim 0.54$  electrons/unit-cell and is consistent with an  $\sim 0.6$  electrons/unit-cell, which is expected for  $(1-x)$  at  $x = 0.4$  from a simple assumption about band structure and atomic valence. The potassium content dependence of  $n_H$  has the same trend as that of a transition temperature  $T_c$  above  $x \sim 0.35$ ;  $T_c$  reaches its maximum value at a potassium content of  $x \sim 0.4$ , where  $n_H$  takes the largest value. In an optical study, Karlow et al. [31] also observed a peak at  $x \sim 0.35$  in the potassium content dependence of an effective carrier number. Moreover, by using tunneling spectroscopy, Kosugi et al. [23] confirmed the validity of weak-coupling BCS relation  $2\Delta/k_B T_c = 3.5$  for the superconducting crystals used in this study. The above facts clearly indicate that BKBO is a conventional BCS-like high- $T_c$  superconductor.

The temperature-dependent Hall coefficient or carrier density has been reported for BKBO crystals [14,37,38]. However, the data show some discrepancies that seem to be due to the quality of the crystals and an uncertainty in composition, including oxygen content. In this study, the temperature dependence of carrier density  $n_H(T)$  was measured for high-quality crystals with distinct potassium

Table 4

The parameters  $n_m$ ,  $n_s$ , and  $T_s$ , which are used for fitting the temperature dependence of Hall density  $n_H$  for crystals with potassium contents of 0.39, 0.43, and 0.56

$x$	$n_m$ ( $\times 10^{21}/\text{cm}^3$ )	$n_s$ ( $\times 10^{21}/\text{cm}^3$ )	$E_s$ (meV)
0.39	4.19	12.4	35
0.43	6.09	1.41	25
0.56	7.39	1.19	1.3

and oxygen contents. Some typical behaviors of  $n_H(T)$  for crystals with superconducting compositions are shown in Fig. 7. The  $n_H$  shows almost linear temperature dependence at temperatures between 150 and 270 K. For a comparison of the variation of  $n_H$  against the temperature,  $n_H(T)$  were fitted roughly by straight lines, and the slope  $dn_H/dT$  of the lines is shown as a function of potassium content  $x$  in the inset of Fig. 7. While  $dn_H/dT$  is significant for a crystal with a composition of  $x \sim 0.4$ , it tends to decrease drastically with increasing potassium content. The  $dn_H/dT$  is very small for crystals of  $x > 0.5$ . The temperature-dependent Hall density observed for crystals with  $x = 0.39$  and 0.43 can be ascribed to the nature of the semiconducting component, which persists in the cubic metallic phase. If semiconducting and metallic components coexist in the crystal, the Hall density will depend on temperature according to the relation  $n_H(T) = n_m + n_s / [\exp(E_s/k_B T) + 1]$ , where  $n_m$  and  $n_s$  are carrier densities of metallic and semiconducting components at 0 K, and  $E_s$  is excitation energy across the band-gap. The  $n_H(T)$  of the crystals with  $x = 0.39$ , 0.43, and 0.56 were fitted by the above equation, and the results are shown by solid lines in Fig. 7.  $n_m$ ,  $n_s$ , and  $E_s$  obtained by the fitting are listed in Table 4. Though the  $E_s$  of the crystals with  $x = 0.39$  and 0.43 are slightly smaller than those obtained from the analysis of  $\rho(T)$ , they are consistent

with those of  $\rho(T)$ . The existence of a semiconducting component may be the reason that temperature-dependent Hall density was observed in BKBO crystals with a high- $T_c$  composition. When the amount of the semiconducting component decreases due to an increase in the doping level, the temperature dependence of the Hall density will disappear. Extremely small  $n_s$  and  $E_s$  of crystals with  $x = 0.56$  implies a disappearance of the semiconducting component or band gap. The carrier density  $n_m$  of the crystals with a metallic composition ( $x > 0.5$ ) is temperature-independent, like conventional metals.

#### 4. Conclusion

The characteristic features of the transport properties in BKBO were investigated by means of resistivity as well as Hall-effect measurements. Possible band schemes for the BKBO system are shown in Fig. 8 for some characteristic potassium composition ranges.  $\text{BaBiO}_3$  is a semiconductor in spite of the fact that band-structure calculations predicted metallic behavior. A half-filled Bi 6s band seems to be electronically unstable. It is split into an empty upper band and a filled lower band with a gap opening at the Fermi level that is due to a strong coupling of lattice distortions of  $\text{BiO}_6$  octahedra and charge fluctuations of the Bi ions. A small doping of potassium into the barium site introduces a structural transformation from a monoclinic to an orthorhombic phase, but the system still behaves as a semiconductor without exhibiting superconductivity. As potassium doping is equivalent to the removal of electrons from a lower Bi 6s band, hole-density increases upon potassium doping at semiconducting compositions ( $0 \leq x < 0.35$ ) and the holes behave as the majority carriers in transport phenomena.

When the potassium content exceeds a critical

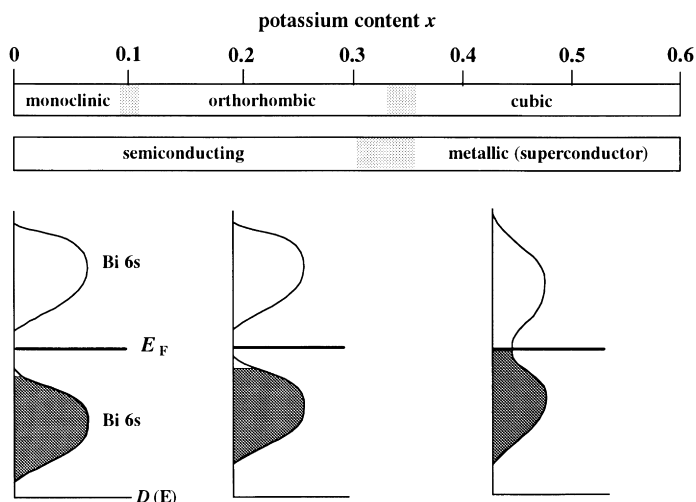


Fig. 8. A possible band scheme of  $\text{Ba}_{1-x}\text{K}_x\text{BiO}_3$  for a variation of potassium content  $x$ .



concentration ( $x \sim 0.35$ ), the material transforms to a cubic phase. The phase transition from an orthorhombic to a cubic structure seems to change the electronic structure of BKBO. A single metallic band is established in the cubic phase, and the material exhibits superconductivity. However, in crystals with a composition in the vicinity of the critical composition  $x \sim 0.35$ , semiconducting and metallic components seem to coexist in a crystal. The maximum transition temperature exceeding 30 K is observed at a composition of  $x \sim 0.4$ , where carrier density has its maximum value. The resistivity of crystals with a metallic composition can be ascribed to the scattering of conduction electrons by phonons with an energy distribution from 20 to 50 meV. This fact implies that a phonon-mediated mechanism plays a key role in the superconductivity of BKBO.

Further doping of potassium introduces holes into the metallic Bi 6s band, and the density of electrons decreases, thereby causing a decrease in  $T_c$ . Superconductivity can be observed up to the composition of solubility limit  $x \sim 0.6$  ( $T_c \sim 8.5$  K). Recently, it has been revealed by X-ray absorption spectroscopy (XAS) measurements for the same crystals as those used in this study that doped holes go into the Bi-6s–O-2p antibonding orbital [39]. This is consistent with the result of Hall effect measurement. If holes are injected into the conduction band, the Fermi level will shift to lower energy. A shift of the Fermi level against potassium doping has been observed in XPS measurements for the same crystals as those used in this study [22,39]. This fact might support the validity of the rigid-band picture assumed in this study. Finally, it is noted that a variable range hopping conduction may exist at compositions of phase boundaries.

### Acknowledgements

The work at Aoyama Gakuin University was supported by a Grant-in-Aid for Scientific Research from the Ministry of Education, Science, Sports and Culture, Japan and by The Science Research Promotion Fund of Japan Private School Promotion Foundation. A part of the work done at Aoyama Gakuin University was supported by a grant from The Research Institute of Aoyama Gakuin University.

### References

- [1] L.F. Mattheis, E.M. Gyorgy, D.W. Johnson Jr., *Phys. Rev. B* 37 (1988) 3745.
- [2] R.J. Cava, B. Batlogg, J.J. Krajewski, R.C. Farrow, L.W. Rupp Jr., A.E. White, K.T. Short, W.F. Peck Jr., T.V. Kometani, *Nature* 332 (1988) 814.
- [3] S. Pei, J.D. Jorgensen, B. Dabrowski, D.G. Hinks, D.R. Richards, A.W. Mitchell, J.M. Newsam, S.K. Sinha, D. Vaknin, A.J. Jacobson, *Phys. Rev. B* 41 (1990) 4126.
- [4] L.F. Mattheis, D.R. Hamann, *Phys. Rev. Lett.* 60 (1988) 2681.
- [5] D.G. Hinks, J.D. Jorgensen, D.R. Richards, S. Pei, Y. Zheng, B. Dabrowski, A.W. Mitchell, *J. Less-Common Metals* 168 (1991) 19.
- [6] Y. Nagata, N. Suzuki, T. Uchida, W.D. Mosley, P. Klavins, R.N. Shelton, *Physica C* 195 (1992) 195.
- [7] G.T. Seidler, T.F. Rosenbaum, P.D. Han, D.A. Payne, B.W. Veal, *Physica C* 195 (1992) 373.
- [8] C. Escribe-Filippini, J. Marcus, M. Affronte, H. Rakoto, J.M. Broto, J.C. Ouset, S. Askenazy, *Physica C* 210 (1993) 133.
- [9] T. Uchida, S. Nakamura, N. Suzuki, Y. Nagata, M.D. Lan, P. Klavins, R.N. Shelton, *Physica C* 215 (1993) 350.
- [10] M. Affronte, J. Marcus, C. Escribe-Filippini, A. Sulpice, H. Rakoto, J.M. Broto, J.C. Ouset, S. Askenazy, A.G.M. Jansen, *Phys. Rev. B* 49 (1994) 3502.
- [11] E.S. Hellman, B. Miller, J.M. Rosamilia, E.H. Hartford, K.W. Baldwin, *Phys. Rev. B* 44 (1991) 9719.
- [12] J. Marcus, C. Escribe-Filippini, S.K. Agarwal, C. Chailout, J. Durr, T. Fournier, J.L. Tholence, *Solid State Commun.* 78 (1991) 967.
- [13] H.Y. Tang, W.L. Chen, T.R. Chien, M.L. Norton, M.K. Wu, *Jpn J. Appl. Phys.* 32 (1993) L312.
- [14] M. Afronte, J. Marcus, C. Escribe-Filippini, *Solid State Commun.* 85 (1993) 501.
- [15] S.F. Lee, J.Y.T. Wei, H.Y. Tang, T.R. Chien, M.K. Wu, W.Y. Guan, *Physica C* 209 (1993) 141.
- [16] M.L. Norton, H.Y. Tang, *Chem. Mater.* 3 (1991) 431.
- [17] J.M. Rosamilia, S.H. Glarum, R.J. Cava, B. Batlogg, B. Miller, *Physica C* 182 (1991) 285.
- [18] Z.J. Huang, H.H. Fang, Y.Y. Xue, P.H. Hor, C.W. Chu, M.L. Norton, H.Y. Tang, *Physica C* 180 (1991) 331.
- [19] P.D. Han, L. Chang, D.A. Payne, *J. Cryst. Growth* 128 (1993) 798.
- [20] W.D. Mosley, J.Z. Liu, A. Matsushita, Y.P. Lee, P. Klavins, R.N. Shelton, *J. Cryst. Growth* 128 (1993) 804.
- [21] H. Takahashi, N. Mhri, Y. Nagata, S. Nakamura, T. Uchida, J. Akimitsu, Y. Tokura, *Physica C* 210 (1993) 485.
- [22] H. Namatame, A. Fujimori, H. Torii, T. Uchida, Y. Nagata, J. Akimitsu, *Phys. Rev. B* 50 (1994) 13674.
- [23] M. Kosugi, J. Akimitsu, S. Uchida, M. Furuya, Y. Nagata, T. Ekino, *Physica C* 229 (1994) 389.
- [24] E.S. Hellman, E.H. Hartford Jr., *Phys. Rev. B* 47 (1993) 11 346.
- [25] M.L. Norton, *Mat. Res. Bull.* 24 (1989) 1391.
- [26] H. Takagi, S. Uchida, S. Tajima, K. Kitazawa, S. Tanaka, *Proceedings of 18th International Conference on Physics of Semiconductors, 1986*, p. 1851
- [27] T. Hashimoto, H. Kawazoe, H. Shimamura, *Physica C* 223 (1994) 131.
- [28] N.F. Mott, E.A. Davis, *Electronic process in non-crystalline materials*, Clarendon Press, Oxford, 1979.
- [29] N. Hamada, S. Massida, A.J. Freeman, J. Redinger, *Phys. Rev. B* 40 (1989) 4442.
- [30] D.T. Marx, P.G. Radaelli, J.D. Jorgensen, R.L. Hitterman, D.G. Hinks, S. Pei, B. Dabrowski, *Phys. Rev. B* 46 (1992) 1144.
- [31] M.A. Karlow, S.L. Cooper, A.L. Kotz, M.V. Klein, P.D. Han, D.A. Payne, *Phys. Rev. B* 48 (1993) 6499.
- [32] H.D. Rosenfeld, T. Egami, in: Y.B. Yam, T. Egami (Eds.), *Lattice effect in high- $T_c$  superconductors*, World Scientific, Singapore, 1992, pp. 105.

- [33] B. Dabrowski, D.G. Hinks, J.D. Jorgensen, R.K. Kalia, P. Vashishta, D.R. Richards, D.T. Marx, A.W. Mitchell, *Physica C* 156 (1988) 24.
- [34] C.K. Loog, P. Vashishta, R.K. Kalia, J. Wei, M.H. Degani, D.G. Hinks, D.L. Price, J.D. Jorgensen, B. Dabrowski, A.W. Mitchell, D.R. Richards, Y. Zheng, *Phys. Rev. B* 45 (1992) 8052.
- [35] P. Samuely, N.L. Bobrov, A.G.M. Jansen, P. Wyder, S.N. Barilo, S.V. Shiryayev, *Phys. Rev. B* 48 (1993) 13904.
- [36] A.I. Golovashkin, A.V. Gudenko, A.M. Tskhovrevov, L.N. Zherikhina, M.L. Norton, *Physica C* 231 (1994) 319.
- [37] S.F. Lee, J.Y.T. Tang, T.R. Chien, M.K. Wu, W.Y. Guan, *Physica C* 209 (1993) 141.
- [38] M. Afronte, J. Marcus, C. Escribe-Filippini, A. Sulpice, H. Rakoto, J.M. Broto, J.C. Ousset, S. Askenazy, A.G.M. Jansen, *Phys. Rev. B* 49 (1994) 3502.
- [39] K. Kobayashi, A. Ino, T. Mizokawa, A. Fujimori, H. Samata, Y. Nagata, F.M.F. de Groot, *Phys. Rev. B* 59 (1999) 15100.